Basic concepts in cardiac arrhythmias

(Ital Heart J 2004; 5 (Suppl 1): 51S-65S)

OBLIGATORY ROLE OF VOLTAGE OSCILLATIONS IN CARDIAC PACEMAKER DISCHARGE

Mario Vassalle

Department of Physiology and Pharmacology, State University of New York, Downstate Medical Center, Brooklyn, NY, USA

When $[K^+]_o$ is suitably increased, all cells of the sino-atrial node (SAN) assume the characteristics of dominant pacemaker action potentials (slow responses with a U-shaped diastolic depolarization). As $[K^+]_o$ is further increased, two oscillatory potentials become visible during diastole, superimposed on diastolic depolarization: the after-potential V_{os} and the pre-potential ThV_{os}. Their role in the initiation and maintenance of pacemaker discharge was studied by means of a microelecrode technique and in Purkinje fibers also by means of a patch-clamp technique. The results obtained are reviewed here. V_{os} obligatorily follows the action potential whereas ThV_{os} can occur at any time during diastole. In the SAN, V_{os} and ThV_{os} become visible in high $[K^+]_o$ because their size decreases and they miss the threshold for the action potential. In Purkinje fibers, ThV_{os} appear in low $[K^+]_o$ and lead to the onset of discharge. In both tissues, as diastolic depolarization enters a less negative voltage range ("oscillatory zone"), ThV_{os} appear, grow in size and attain the threshold. During recovery, ThV_{os} occur sooner in diastole and fuse with V_{os}: both oscillations increase in size and accelerate SAN discharge. In high $[K^+]_o$, high $[Ca^{2+}]_o$, fast drive and norepinephrine increase the size and slope of V_{os} and of ThV_{os}, which in turn restore or accelerate discharge. In contrast, low $[Ca^{2+}]_o$, high $[Ni^{2+}]$ and cholinergic agonists decrease V_{os} and ThV_{os} and cause SAN arrest. Low $[Ni^{2+}]$ (35.5 μM) increases the rate whereas ryanodine has the opposite effect. Thus, ThV_{os} and V_{os} play an obligatory role in the initiation and maintenance of SAN discharge, V_{os} by steepening early diastolic depolarization and ThV_{os} by attaining the threshold in dominant pacemaker range. ThV_{os} have a similar role in Purkinje fibers. In the SAN, both V_{os} and ThV_{os} are Ca^{2+}-dependent and are regulated by autonomic mediators whereas in Purkinje fibers ThV_{os} are due to a slowly inactivating sodium current (I_{Na3}). Thus, ThV_{os} and V_{os} are caused by different mechanisms and they link diastolic depolarization to the threshold, thereby playing an essential role in the discharge and autonomic control of cardiac pacemakers.

Introduction

Diastolic depolarization (DD) is needed for pacemaker discharge, but additional events appear necessary for spontaneous activity. Evidence will be reviewed which indicates that diastolic voltage oscillations exist which are not only needed for the initiation, but also for the maintenance of spontaneous discharge both in the sino-atrial node (SAN) and in Purkinje fibers. Under normal circumstances, these diastolic oscillations (V_{os} and ThV_{os}, in the SAN and ThV_{os} in Purkinje fibers) are fused with the early diastolic depolarization (DD_1) and therefore are not visible, but they become apparent when $[K^+]_o$ is suitably varied. The aim of this presentation is to review the pertinent evidence that demonstrates the obligatory role of V_{os} and ThV_{os} in the discharge of cardiac pacemakers. Also, these oscillations appear to play a role in autonomic control.

Methods

The studies were carried by using microelectrode techniques in Purkinje strands and isolated SAN as well as in single Purkinje cells with patch-clamp techniques. The methods used are described in details in the publications that will be quoted for the different results.

Results and discussion

The oscillatory pre-potentials ThV_{os} in Purkinje fibers. *Initiation of spontaneous discharge.* In Purkinje fibers, when $[K^+]_o$ is

lowered from 5.4 to 2.7 mM voltage oscillations appear (ThV_{os}) that swing above and below the resting potential, increase in size, and attain the threshold. As ThV_{os} shift to a more negative value and increase in size, the threshold for the action potential (AP) is reached sooner. When ThV_{os} become completely fused with DD_1, they are no longer visible[1]. At that stage, DD proceeds from the maximum diastolic potential to the threshold[1-4]. When a slow discharge is initiated by ThV_{os}, the AP is not followed by ThV_{os}[1-3]. ThV_{os} again appear when DD progresses into a less negative voltage range ("oscillatory zone"). If ThV_{os} fail to attain the threshold, their succession becomes "diamond-shaped": they increase to a maximum and then gradually decrease to the resting potential. Thus, the depolarizing phase of ThV_{os} is the link between DD and threshold for the upstroke and it mediates the initiation of discharge.

The disappearance of ThV_{os} after an AP is due to the hyperpolarization to the maximum diastolic potential, which is negative to the "oscillatory zone". This is demonstrated by the fact that a small decrease of the resting potential by Ba^{2+} induces ThV_{os} and a small hyperpolarization by Cs^+ suppresses them (Fig. 1)[2]. Cs^+ hyperpolarizes the membrane through the stimulation of the Na^+-K^+ pump activity[5].

Maintenance of spontaneous discharge. If $[K^+]_o$ is low enough, ThV_{os} appear progressively sooner during diastole until they fuse with V_{os} (if present) and DD_1. At that point, V_{os} and ThV_{os} are no longer visible and DD_1 appears to directly attain the threshold. However, that ThV_{os} are the link between DD and threshold also during continuous discharge is shown by re-increasing $[K^+]_o$. The sudden failure of DD to attain the threshold unmasks a ThV_{os} which is followed by another one that (being larger) attains the threshold. As, overall, ThV_{os} gradually decrease in amplitude, it takes longer for them to increase sufficiently to reach the threshold and the rate continues to decrease. Eventually, ThV_{os} consistently miss the threshold and the "diamond pattern" appears which is followed by quiescence.

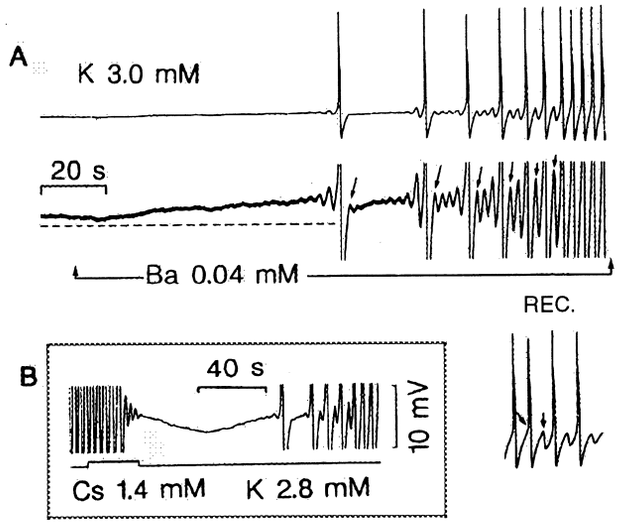

Figure 1. *Shift of the resting potential into and out of the oscillatory zone in a Purkinje fiber. In* A, *action potentials* (top strip) *and their lower part* (lower strip) *are shown. Ba^{2+} decreased the resting potential and allowed ThV_{os} to appear. In* panel labeled REC. *(recovery), the slowing of discharge was due to ThV_{os} missing the threshold. In* boxed inset B, *Cs^+ unmasked ThV_{os} and caused a transient hyperpolarization negative to the oscillatory zone. From Spiegler and Vassalle[2], modified.*

The oscillatory after-potential V_{os} and pre-potential ThV_{os} in the sino-atrial node. Under normal conditions, also in the SAN, the oscillatory potentials are not visible. However, when $[K^+]_o$ is increased, the maximum diastolic potential decreases and all APs assume dominant-like configuration (slow responses with U-shaped DD). Although the SAN is much more resistant than Purkinje fibers to high $[K^+]_o$[6,7], when $[K^+]_o$ is further increased, V_{os} and ThV_{os} size decreases[6,7]. When V_{os} and ThV_{os} miss the threshold, their role in the maintenance of discharge is unmasked (Fig. 2a-c). As ThV_{os} occur later during diastole, they become separated from V_{os} which remains superimposed on DD_1 (Fig. 2d). If ThV_{os} consistently miss the threshold, they assume the "diamond patterns", decrease in size, disappear and quies-

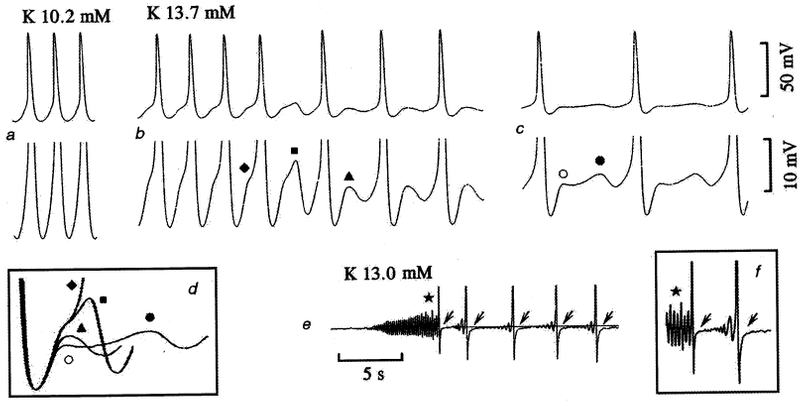

Figure 2. *Unmasking and separation of V_{os} and ThV_{os}. The traces labeled with* a diamond, square, triangle (panel b), empty circle *and* dot (panel c) *have been superimposed in* boxed inset d. *In* panel e, *the star marks increasing ThV_{os} that led to spontaneous discharge.* Arrows *point to temporary suppression of ThV_{os} after each action potential. Thin* line *emphasizes negative shift of ThV_{os}.* Boxed inset f *shows part of e trace at higher gain. From Nett and Vassalle[7], modified.*

cence follows. Apparently, in SAN dominant pacemakers, DD is due to the superimposition of fused DD_1, V_{os} and ThV_{os}.

On lowering $[K^+]_o$, the initiation of discharge is due to appearance of gradually increasing ThV_{os} that attain the threshold (Fig. 2e): the AP thus induced temporarily suppresses ThV_{os}, which again appears only when DD enters the oscillatory zone. Indeed, if sub-threshold ThV_{os} are continuously present in an otherwise quiescent SAN, a driven AP leads to the temporary suppression of ThV_{os}. This behavior of ThV_{os} is similar to that in Purkinje fibers. V_{os} exists also in Purkinje fibers, but usually under conditions of Ca overload (e.g., digitalis toxicity).

On further reduction of high $[K^+]_o$, ThV_{os} occur progressively earlier during DD and fuse with V_{os}: when that happens, V_{os} and ThV_{os} cease to be visible and DD appear to continue directly into the upstroke (U-shaped DD). During recovery in Tyrode solution, size and slope of V_{os} and of ThV_{os} markedly increase and cause a faster discharge. As APs assume the subsidiary configuration with a more negative maximum diastolic potential, there is an abrupt transition between their DD and the upstroke[7]. Subsidiary DD is well negative to the oscillatory zone and ThV_{os} would be suppressed. The presence of ThV_{os} in dominant and their absence in the subsidiary range may be a major characteristic that differentiate dominant from subsidiary pacemakers[7].

Thus, V_{os} and ThV_{os} are separate voltage oscillations that play an obligatory role in the initiation and maintenance of SAN discharge, V_{os} by increasing size and slope of DD_1 and ThV_{os} by attaining the threshold in dominant pacemaker range, either by increasing during late DD at slow rates or by fusing with V_{os} at fast rates.

Mechanism of induction of ThV_{os} on lowering $[K^+]_o$. In suitably high $[K^+]_o$, both the SAN and Purkinje fibers are quiescent (although the SAN requires much higher $[K^+]_o$). In both tissues, lowering $[K^+]_o$ leads to the appearance of ThV_{os} through an undetermined mechanism. One possible factor may be the decrease in Na^+-K^+ pump activity: in Purkinje fibers, a lower $[K^+]_o$ increases the intracellular Na activity (a^i_{Na})[8]. As a consequence, $[Ca^{2+}]_i$ also increases through the Na-Ca exchange: contractile force does increase in lower $[K^+]_o$[3,7]. In turn, an increase in $[Ca^{+2}]_i$ increases DD slope and amplitude[7,9] and also shifts the oscillatory zone in a negative direction[3,7].

A larger DD may enter the oscillatory zone, especially in view of the negative shift of the latter. These changes would lead to the onset of ThV_{os}. Higher $[Ca^{2+}]_i$ may shift the oscillatory zone by screening the negative changes at the inner side of the plasma membrane.

In Purkinje fibers, high $[Ca^{2+}]_o$ also increases the slope and size of DD_1 and ThV_{os}, thereby facilitating spontaneous discharge[2,3]. That high $[Ca^{2+}]_o$ acts by increasing $[Ca^{2+}]_i$ is supported by the fact that overdriving sheep Purkinje fibers in Tyrode solution also increases DD_1 slope and magnitude and may lead to spontaneous discharge ("overdrive excitation")[10]. The situation is not different in the SAN, since in high $[K^+]_o$, a high $[Ca^{2+}]_o$ or overdrive increases DD and the size of ThV_{os}, which occur progressively sooner during DD and at more negative values[7].

In contrast, low $[Ca^{2+}]_o$ and millimolar concentrations of Ni^{2+} abolish V_{os} and ThV_{os} and cause SAN arrest[7]. ThV_{os} are unrelated to Ca sparks that appear during the late DD and are caused by $I_{Ca,T}$, since a micromolar concentration of Ni^{2+} not only does not stop the SAN, but in fact increases its rate[7]. In high $[K^+]_o$ (the Na-K pump is already stimulated) Cs^+ induces or accelerates discharge as ThV_{os} increase in size and reach the threshold sooner[6]. Therefore, ThV_{os} and initiation of activity in the SAN do not appear to involve I_f which is blocked by Cs^+.

Ionic current underlying the depolarizing phase of ThV_{os}. The current underlying the depolarizing phase of ThV_{os} has to be net inward. In spontaneously discharging Purkinje fibers, the last part of DD undergoes an upward swing which presumably is due to the depolarizing phase of ThV_{os}. Tetrodotoxin (TTX), a blocker of Na^+ channels, suppresses the upward concavity at a time when it has little effect on the initial DD (Fig. 3)[11]. As a consequence, DD misses the threshold and quiescence follows[4]. If ThV_{os} are inducing a slow discharge, TTX suppress them and leads to quiescence[2].

Patch-clamp experiments in single Purkinje cells show that the current underlying the depolarizing phase of ThV_{os} is a slowly inactivating Na^+ current[12]. In figure 4, during the -58 mV step, a slowly decaying inward component (labeled I_{Na3}, dot) appeared, which increased in size during the -56 mV step. During the -52 mV step, the fast Na^+ current I_{Na} quickly activated and inactivated (see trace at normal gain) and was not followed by a slowly decaying current (see I_{Na} at high gain), as previously reported[13,14]. During the -40 mV step, I_{Na} inactivation was interrupted by another slowly decaying inward component which became larger at -32 mV (labeled I_{Na2}, square). I_{Na2} was larger and decayed more slowly than I_{Na3} and it was incompletely inactivated by the end of the 500 ms step (see boxed inset)[12]. I_{Na3} and I_{Na2} are independent currents and not slowly inactivating fractions of I_{Na}[12,14].

During depolarizing ramps that do not elicit I_{Na}, the current undergoes inward rectification with a negative slope region that begins at ~ -60 mV and peaks at ~ -35 mV and is larger during faster ramps. Increasing diphasic ("oscillatory") voltage ramps require much smaller currents at V_h -60 mV than at V_h -80 mV and are associated with a marked decrease in slope conductance (inward rectification). At V_h -50/-40 mV, the oscillatory ramp currents and superimposed pulse currents reverse direction due to the negative slope. Low $[K^+]_o$ (2.7 mM) reduces the steady state slope conductance as well as the

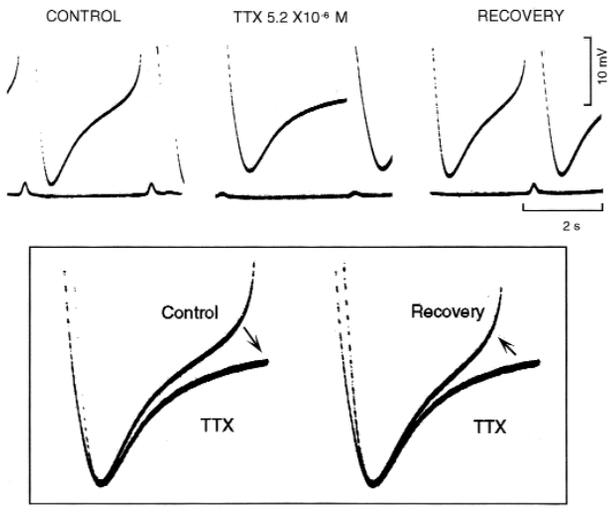

Figure 3. *Tetrodotoxin (TTX) suppresses the last part of diastolic depolarization in Purkinje fibers. The fiber was spontaneous active in control, driven in the presence of TTX and spontaneous again during recovery. In the boxed inset, the trace recorded in the presence of TTX was superimposed on control and recovery traces. From Vassalle[11], by permission of the Martinus Nijhoff Publishers.*

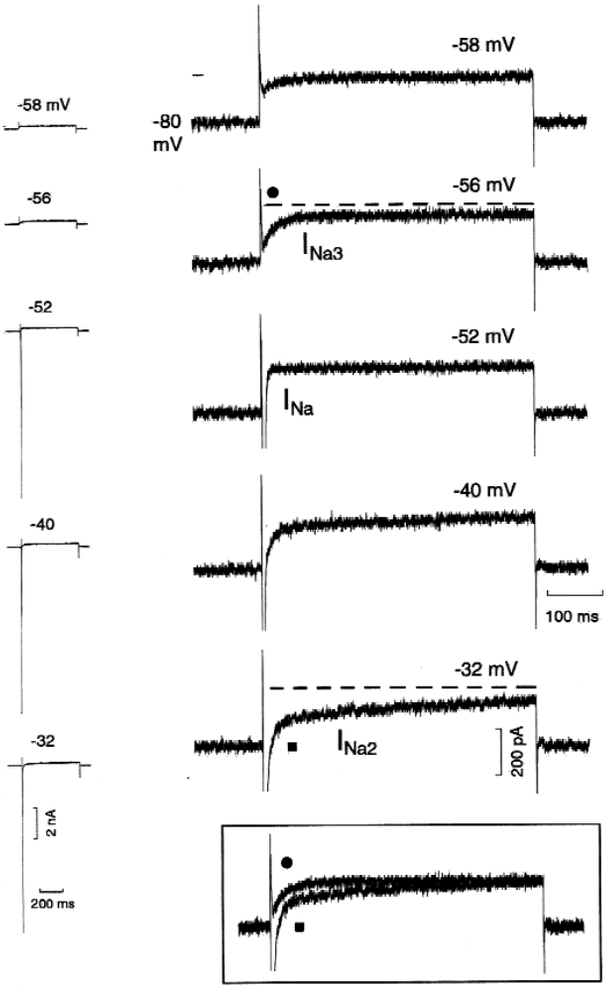

Figure 4. *Different Na components during depolarizing steps to different values. The current traces during depolarizing steps are shown on the* left side *of the figure and at higher gain on the* right side *of the figure. The* dashed lines *emphasize the decay of* I_{Na3} (dot) *and* I_{Na2} (square). I_{Na2} *and* I_{Na3} *traces are superimposed in the* boxed inset *(same respective symbol). From Rota and Vassalle[12], by permission of The Physiology Society.*

current in the diastolic range, and increases (as well as shifts in a negative direction) I_{Na3}. High $[K^+]_o$ has the opposite effects. Cs^+ (2 mM) and Ba^{2+} (2 mM) reduce the initial current during depolarizing ramps, but not I_{Na3}. In current-clamp mode, current-induced voltage oscillations elicit APs through a gradual transition between DD and upstroke, consistent with the activation of I_{Na3}. Thus, the initiation and maintenance of spontaneous discharge in Purkinje strands appear to involve a voltage- and K^+-dependent decrease in K^+ conductance as well as the activation of a voltage- and time-dependent inward Na^+ current (I_{Na3}) with slow inactivation kinetics.

If I_{Na3} is caused by current flow through Na^+ channel, TTX would be expected to block it. In figure 5, the protocol is shown in panel C, and in panel A the current traces are shown in control, in the presence of TTX and during recovery. TTX increased the current in an outward direction, markedly reduced the amplitude of I_{Na3} during the initial ramp (see traces at higher gain in the top boxed inset, K^+ 4 mM, vertical arrows) as well as its subsequent slow decay (gray areas in A), and abolished the reversal of current direction during the oscillatory ramps (see bottom boxed inset). During the TTX washout, the changes subsided. Similar results were obtained with lidocaine (100 μM).

In figure 5B, lower (2.7 mM) $[K^+]_o$ increased the negative slope and shifted it in an inward direction (cf. first panels in A and B). Adding TTX induced changes similar to those in 4 mM $[K^+]_o$. In particular, TTX markedly decreased I_{Na3} (see top boxed inset, K^+ 2.7 mM, oblique arrows) and its subsequent decay (panel B). When small hyperpolarizing pulses were superimposed on the C protocol (Fig. 5D) the following was obtained: 1) a decrease in the amplitude of the pulse currents due to inward rectification (dot); 2) the reversal of the superimposed pulse currents in the negative slope range (filled and empty squares); 3) increasing amplitude of the reversed pulse currents during the negative slope, indicating an increase in conductance; 4) the appearance of a slowly decaying inward transient after the hyperpolarizing pulses (filled and empty squares), due to a partial recovery of I_{Na3}; and 5) a subsequent gradual decrease of the amplitude of the reversed pulses due to inactivation of I_{Na3}.

Although in the SAN the behavior of ThV_{os} is quite similar to that in Purkinje fibers, the current responsible for the depolarizing phase of ThV_{os} is unlikely to be the same, due to the little effect of TTX on SAN dominant pacemakers and the sensitivity of ThV_{os} to $[Ca^{2+}]_o$[7]. Therefore, Ca^{2+} is likely to play in the depolarizing phase of ThV_{os} of the SAN the role that I_{Na3} plays in the ThV_{os} of Purkinje fibers.

Ionic mechanism underlying V_{os}. In Purkinje fibers, the mechanism underlying V_{os} is related to Ca^{2+} overload of the sarcoplasmic reticulum[9,15]. A Ca^{2+} overloaded sarcoplasmic reticulum releases Ca^{2+} also in diastole[15]. The release is oscillatory (it starts, peaks and decays) and induces both an aftercontraction and V_{os}. V_{os} is due to

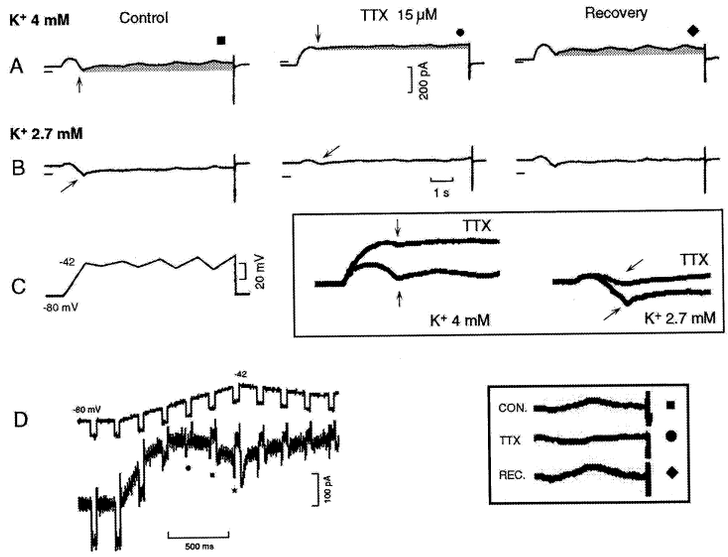

Figure 5. *Effects of tetrodotoxin (TTX) on I_{Na3}. The traces recorded in control, in the presence of TTX and during recovery are shown in* A *(4 mM $[K^+]_o$) and in* B *(2.7 mM $[K^+]_o$). The effects of TTX on the negative slope are shown at higher gain in the* boxed inset *in* C, *the same* arrows *identifying the same traces within and without the inset. In A, the* gray areas *emphasize the slow decay of I_{Na3} and the reduction of its amplitude by TTX. The* boxed inset *in* D *shows at higher gain the abolition by TTX of the reversal of the current direction during the last oscillatory ramps. The* first D panel *was recorded from another cell in Tyrode solution: the* top trace *shows the voltage protocol and the* bottom trace *the current trace. The* dot, *the* filled *and the* empty squares *identify step currents with different characteristics. From Rota and Vassalle[12], by permission of The Physiology Society.*

electrogenic extrusion of Ca^{2+} released by the sarcoplasmic reticulum in diastole through the Na^+-Ca^{2+} exchange, thereby creating an inward current (I_{os})[15]. A sufficiently large V_{os} may attain the threshold and initiates an AP or a train of APs.

In the SAN, the presence of V_{os} even in high $[K^+]_o$ (which decreases Ca^{2+} influx and force[7]) might be due to the sparseness of the sarcoplasmic reticulum and a smaller driving force for Ca^{2+} extrusion (the dominant diastolic potential is less negative than in other cardiac tissues)[7]. Therefore, Ca^{2+} would tend to accumulate in the sarcoplasmic reticulum. As in Purkinje fibers[15], also in the SAN, V_{os} increases when the Ca^{2+} load increases (high $[Ca^{2+}]_o$, fast drive[7]) and decreases when the Ca^{2+} load decreases and in the presence of ryanodine[7].

Regulation of diastolic oscillations by neuromediators. Norepinephrine decreases the resting potential and induces ThV_{os} that initiate discharge both in Purkinje fibers and the SAN. Norepinephrine also accelerates the SAN through the earlier onset of larger ThV_{os}. Instead, cholinergic agonists decrease the size of both V_{os} and ThV_{os}, thereby slowing the rate and eventually causing SAN standstill. Higher concentrations also cause a marked hyperpolarization[16]. Therefore, it appears that diastolic oscillations play a major role in the control of SAN discharge by the autonomic system.

General conclusions

DD is the mechanism by which the membrane potential decreases from the maximum diastolic potential to the oscillatory zone, where the induction of ThV_{os} leads to the attainment of the threshold. Therefore, ThV_{os} are indispensable for spontaneous discharge of dominant SAN pacemakers and of Purkinje fibers. V_{os} steepens DD_1 and (if large enough) enters the oscillatory zone and fuses with ThV_{os}. V_{os} appears to contribute to fast discharge of the SAN under normal circumstances and to that of Purkinje fibers under abnormal circumstances.

Acknowledgments

The work cited in this paper from the laboratory of the author was supported by grants from NIH and from the American Heart Association, New York Affiliate.

References

1. Vassalle M. Cardiac pacemaker potentials at different extra- and intracellular K concentrations. Am J Physiol 1965; 208: 770-5.
2. Spiegler P, Vassalle M. Role of voltage oscillations in the automaticity of sheep cardiac Purkinje fibers. Can J Physiol Pharmacol 1995; 73: 1165-80.
3. Berg DE, Vassalle M. Oscillatory zones and their role in normal and abnormal sheep Purkinje fiber automaticity. J Biomed Sci 2000; 7: 364-79.
4. Vassalle M, Scidà EE. The role of sodium in spontaneous discharge in the absence and in the presence of strophanthidin. (abstr) Fed Proc 1979; 38: 880.
5. Iacono G, Vassalle M. The relation between cesium, intracellular sodium activity and pacemaker potential in cardiac Purkinje fibers. Can J Physiol Pharmacol 1990; 68: 1236-46.
6. Kim EM, Choy Y, Vassalle M. Mechanisms of suppression and initiation of pacemaker activity in guinea pig sino-atrial node superfused in high $[K^+]_o$. J Mol Cell Cardiol 1997; 29: 1433-45.

7. Nett MP, Vassalle M. Obligatory role of diastolic voltage oscillations in sino-atrial node discharge. J Mol Cell Cardiol 2003; 35: 1257-76.
8. Abete P, Vassalle M. Role of intracellular Na^+ activity in the negative inotropy of strophanthidin in cardiac Purkinje fibers. Eur J Pharmacol 1992; 211: 399-409.
9. Tamargo J, Vassalle M. Mechanisms by which calcium modulates diastolic depolarization in sheep Purkinje fibers. J Electrocardiol 1991; 24: 349-61.
10. Choi WS, Vassalle M. Mechanisms by which discharge modulates diastolic depolarization in sheep and dog Purkinje fibers. J Electrocardiol 2002; 35: 253-72.
11. Vassalle M. The role of the slow inward current in impulse formation. In: Zipes DP, Bailey JC, Elharrar V, eds. The slow inward current and cardiac arrhythmias. The Hague: Martinus Nijhoff Publishers, 1980: 127-48.
12. Rota M, Vassalle M. Patch-clamp analysis in canine cardiac Purkinje cells of a novel sodium component in the pacemaker range. J Physiol 2003; 548 (Part 1): 147-65.
13. Vassalle M, Du F. A slow sodium current in single Purkinje cells. (abstr) FASEB J 2000; 14: A699.
14. Bocchi L, Vassalle M. An analysis of the slow sodium current in single Purkinje and myocardial cells. (abstr) FASEB J 2000; 14: A699.
15. Vassalle M, Mugelli A. An oscillatory current in sheep cardiac Purkinje fibers. Circ Res 1981; 48: 618-31.
16. Catanzaro JN, Nett MP, Rota M, Vassalle M. Role of diastolic oscillations in the autonomic control of the sino-atrial node. FASEB J 2004, in press.

SEROTONIN AND ATRIAL NATRIURETIC PEPTIDE MODULATE THE PACEMAKER CURRENT: A POSSIBLE LINK WITH ARRHYTHMOGENESIS

Giuseppe Lonardo, Raffaele Paola, Francesca Stillitano, Laura Sartiani, Simona Brogioni, Alessandro Mugelli, Elisabetta Cerbai

Center of Molecular Medicine (CIMMBA), University of Florence, Florence, Italy

Introduction

Chronic atrial fibrillation is the most common cardiac arrhythmia in clinical practice. The interest in understanding the molecular basis of atrial fibrillation increased over the last years, and is related to both its prevalence, and the fact that prevention and treatment of atrial fibrillation remains inadequate.

Several humoral endogenous factors may favor the appearance of atrial arrhythmias by modulating the electrophysiological properties of human atrial myocytes (HuAM). Catecholamines and serotonin (5-hydroxytryptamine - 5-HT) are considered key factors in this setting. Particularly, a 5-HT receptor subtype, the 5-HT4 one, is uniquely present in the human and pig atrium and absent in common laboratory animals, and it has been suggested that locally released 5-HT from platelets may exert a proarrhythmic action by increasing cell automaticity through the stimulation of this receptor[1]. Beta-adrenergic and 5-HT4 receptors share a common signaling pathway: they increase the intracellular cAMP concentration via stimulation of adenylate cyclase[2,3] (Fig. 1). In the last years, we have been studying the properties of the hyperpolarization-activated channel (I_f) in HuAM, where it is constitutively present[3,4]. These channels belong to the hyperpolarization-activated cyclic nucleotide gated (HCN) family and are directly modulated by cyclic nucleotides[5]. Thus, under appropriate conditions, I_f may play an active role in driving the transmembrane potential toward the threshold of sodium channels, initiating an action potential[6].

The atrial natriuretic peptide (ANP) is an emerging regulator of cardiac functions in physiological and pathological conditions. ANP is released from HuAM by mechanical distension and acts on cardiomyocytes via stimulation of different natriuretic peptide receptor (NPR) subtypes[7]. Two of them (NPR A and B) have a guanylate cyclase activity, and their stimulation causes an increase in intracellular cGMP[7]. Interestingly, cGMP has been shown to stimulate I_f and increase the spontaneous rate of the sino-atrial node[8]. However, no evidence exists about a direct or indirect effect of human ANP on I_f in the human heart (Fig. 1). The aim of this study was to investigate the effect of hormonal triggers on I_f and to evaluate the underlying metabolic pathways.

Methods

Patients. The procedure has been approved by the local medical ethics committee, and informed consent was obtained from all patients before entering the study. The investigation conforms to the principles outlined in the Declaration of Helsinki[9]. A small portion of the right atrial appendage, which is routinely excised for

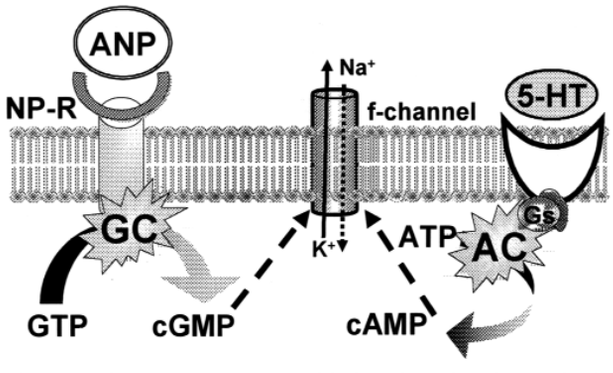

Figure 1. *Schematic representation of the hypothetical mechanism for the action of atrial natriuretic peptide (ANP) and serotonin (5-HT) on I_f. AC = adenylate cyclase; ATP = adenosine triphosphate; cAMP = cyclic adenosine monophosphate; cGMP = cyclic guanosine monophosphate; GC = guanylate cyclase; Gs = stimulatory G protein; GTP = guanosine triphosphate; NP-R = natriuretic peptide receptor.*

allowing extracorporeal circulation, is obtained in the surgery theater. Samples are either immediately placed in a sterile vial and frozen in liquid nitrogen for polymerase chain reaction (PCR) assay, or placed in a vial containing a cold sterile saline solution and immediately transported to the laboratory for cell isolation.

Isolation of human atrial myocytes and patch-clamp experiments. HuAM are isolated from atrial tissue samples following a procedure which has been previously described[3,4]; the patch-clamp technique (whole-cell and perforated-patch recording) was used. Cells were superfused with a normal Tyrode solution; a modified Tyrode solution was used to measure I_f. For the experiments with drug application, the patch-clamped cells were superfused by means of a temperature-controlled micro-superfusor which allows rapid changes in the solution bathing the cell; this enabled us to minimize current run-down and to reduce exposure to drugs of the other cells present in the experimental chamber. 5-HT (0.1-3 μM) or the selective agonist BIMU-8 (1-10 μM) were used for 5-HT4 stimulation. Human ANP was used at 0.1 to 10 nM concentrations.

Measurement of mRNA levels for HCN isoforms by quantitative polymerase chain reaction. Atrial tissue was rapidly weighed and frozen immediately in liquid nitrogen. Total RNA was extracted from human atrial tissue using a Qiagen kit. Frozen tissue was first disrupted and homogenized; ethanol was then added to the lysate, creating conditions which promote selective binding of RNA to the RNeasy membrane. The sample was then applied to the RNeasy minispin column. Total RNA binds to the membrane, contaminants are efficiently washed away, and high-quality RNA is eluted in 30 μl, or more, of RNase-free water. The total RNA was separated by gel electrophoresis and spectrophotometry at 260 and 280 nm was performed to measure the amount and quality of RNA. For the quantitative analysis of human HCN isoforms, the "real-time PCR" approach was used; the technique consists in the simultaneous amplification of target sequences (e.g. HCN2) and of a "reference" (housekeeping-HK) gene (GAPDH); the cleavage of hydrolysis probes due to the 5' exonuclease activity of Taq polymerase allowed for the generation of target-specific fluorescence, which was followed by a "real-time PCR instrument", the Abi Prism 7700 (Applied Biosystems). The instruments allowed the simultaneous detection of the targets in the same tube, so that all samples were run together with their HK gene. Results were analyzed and plotted by using Microsoft Excel software.

Results and discussion

In basal conditions, the threshold for the activation of I_f in HuAM is around -60 mV (Fig. 2A, dotted line); thus, If contributes little to membrane resting potential which lies near -75 mV in these cells. In this respect, the properties of atrial I_f[4] differ from those found in the human ventricular myocytes, where current activation occurs at potentials which are more positive (10-15 mV) than in HuAM[10]. However, stimulation of beta-adrenergic[4] or 5-HT4 receptors[3] can shift the activation curve toward less negative potentials, thus increasing the influence of I_f on membrane potential.

The features of I_f in different cardiac and extracardiac tissues may reside in the molecular properties of the channel. Four different isoforms (HCN1-HCN4) have been cloned in mammalians, whose distribution varies, among species, according to several factors such as tissue, pathological conditions and age[5]. A characterization of atrial isoforms is in progress in our laboratory by means of the real-time PCR technique. Figure 2B shows a typical semi-logarithmic plot for the HCN2 isoform (which is the most abundant in the human atrium) and the HK gene GAPDH, in the same sample analyzed with this technique. Normalization of curves (HCN2 vs GAPDH) gives a value which is directly proportional to the mRNA expression for this particular isoform. Thus, it would be possible to obtain a precise assessment of the relative proportion of HCN isoforms in the atrium.

We tested the action of modulating factors on I_f recorded in HuAM. Figure 3 shows the effect of 5-HT

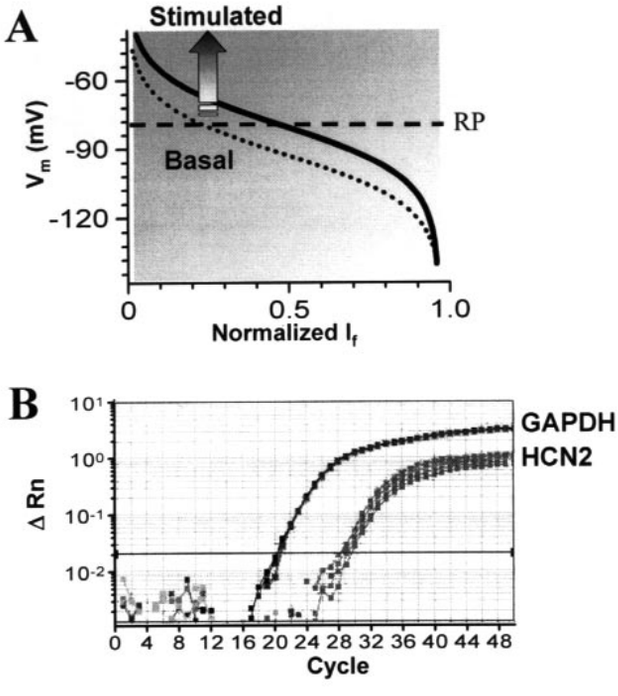

Figure 2. Panel A: *activation curve of If in basal and stimulated conditions. Stimulation by intracellular cyclic nucleotides causes a positive shift of the activation curve, thus increasing I_f amplitude at voltages near the resting membrane potential (RP).* Panel B: *semi-logarithmic view of amplification plot. The line indicates the threshold fluorescence, and it corresponds to the cycle (threshold cycle) at which a significant fluorescence is detected for the target gene (HCN2). Curves are from a typical experiment, run in quadruplicate, for a human atrial sample where HCN2 and GAPDH were tested.*

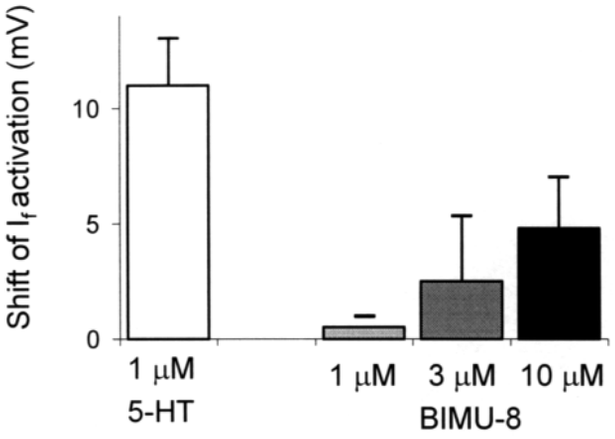

Figure 3. *Effect of serotonin (5-HT) and BIMU-8, a 5-HT4 agonist, on I_f. The effect is expressed as a shift in the activation curve.*

and a selective 5-HT4 agonist, BIMU-8, on the current: the effect is measured as the positive shift of the activation curve. 5-HT causes a 10 mV positive shift[3] similar to that observed for beta-adrenergic stimulation[4]. Also BIMU-8 shifted the I_f activation curve, but it appeared to be less potent than 5-HT. This finding is in agreement with previous data suggesting that BIMU-8 acts as a partial agonist on 5-HT4 human atrial receptors[2,11]. An effect similar to that observed with 5-HT was obtained in HuAM challenged with nanomolar concentrations of human ANP, comparable with the plasma concentration of human ANP reported in patients with chronic atrial fibrillation[12]. Thus, it appears that the intracellular increase in either cAMP or cGMP may modulate I_f, by increasing its amplitude at physiologically relevant potentials.

Pharmacological modulation of I_f may influence its pathophysiological role. In conclusion, our results suggest that locally released factors, originating from activated platelets (5-HT) or stretched cardiomyocytes (ANP), can influence cell electrogenesis. These mechanisms imply a complex relationship between alterations in atrial distension, platelet function and arrhythmogenesis. Through an auto- or paracrine action, human ANP and 5-HT may exert a direct effect on I_f which is constitutively expressed in HuAM. The depolarizing shift in the activation curve of I_f, produced by these substances, might in turn increase its influence on the diastolic membrane potential, and be translated into an increased propensity to spontaneous activity of HuAM[13].

Acknowledgments

Supported by grants from MIUR (COFIN 2002, A. Mugelli). Human biopsies were kindly provided by the Cardiosurgery Unit of Florence (Dr. P.L. Stefano, G. Giunti, B. Fiorani).

References

1. Kaumann AJ. Do human atrial 5-HT4 receptors mediate arrhythmias? Trends Pharmacol Sci 1994; 15: 451-5.
2. Ouadid H, Seguin J, Dumuis A, Bockaert J, Nargeot J. Serotonin increases calcium current in human atrial myocytes via the newly described 5-hydroxytryptamine 4 receptors. Mol Pharmacol 1992; 41: 346-51.
3. Pino R, Cerbai E, Calamai G, et al. Effect of 5-HT4 receptor stimulation on the pacemaker current I_f in human isolated atrial myocytes. Cardiovasc Res 1998; 40: 516-22.
4. Porciatti F, Pelzmann B, Cerbai E, et al. The pacemaker current I_f in single human atrial myocytes and the effect of beta-adrenoceptor and A1-adenosine receptor stimulation. Br J Pharmacol 1997; 122: 963-9.
5. Ludwig A, Zong X, Hofmann F, Biel M. Structure and function of cardiac pacemaker channels. Cell Physiol Biochem 1999; 9: 179-86.
6. Ranjan R, Chiamvimonvat N, Thakor NV, Tomaselli GF, Marban E. Mechanism of anode break stimulation in the heart. Biophys J 1998; 74: 1850-63.
7. Venugopal J. Cardiac natriuretic peptides - hope or hype? J Clin Pharm Ther 2001; 26: 15-31.
8. Musialek P, Lei M, Brown HF, Paterson DJ, Casadei B. Nitric oxide can increase heart rate by stimulating the hyperpolarization-activated inward current, I_f. Circ Res 1997; 81: 60-8.
9. World Medical Association Declaration of Helsinki. Ethical principles for medical research involving human subjects. JAMA 2000; 284: 3043-5.
10. Cerbai E, Pino R, Porciatti F, et al. Characterization of the hyperpolarization-activated current, I_f, in ventricular myocytes from human failing heart. Circulation 1997; 95: 568-71.
11. Langlois M, Fischmeister R. 5-HT4 receptor ligands: applications and new prospects. J Med Chem 2003; 46: 319-44.
12. Rossi A, Enriquez-Sarano M, John C, Lerman A, Abel MD, Seward JB. Natriuretic peptide levels in atrial fibrillation: a prospective hormonal and Doppler-echocardiographic study. JAMA 2000; 35: 1256-62.
13. Opthof T. The membrane current (I_f) in human atrial cells: implications for atrial arrhythmias. Cardiovasc Res 1998; 38: 537-40.

OVEREXPRESSING THE I_f CURRENT AS A THERAPEUTIC STRATEGY TO COMPENSATE FOR ATRIOVENTRICULAR BLOCK

Richard B. Robinson, Peter R. Brink*, Ira S. Cohen*, Michael R. Rosen

*Department of Pharmacology and Center for Molecular Therapeutics, Columbia University, New York, NY, *Department of Physiology and Biophysics, State University of New York at Stony Brook, Stony Brook, NY, USA*

A number of laboratories have begun exploring gene- and cell-based strategies for creation of a biological pacemaker, intended as an eventual substitute for the current generation of implantable electronic pacemakers. Our research has focused on assessing the feasibility of using members of the pacemaker channel gene family (HCN) as the source of depolarizing current in a biological pacemaker. We have overexpressed the HCN2 gene in the canine heart *in situ,* either by gene delivery to myocardial cells or by implantation of an over-

expressing cell population into the myocardium. We have found that, by either delivery method, the overexpressed HCN2 channel generates an ectopic focus that is capable of driving the heart when normal sinus rhythm is suppressed.

Implantable electronic pacemakers are a common therapeutic modality for treating atrioventricular block and other cardiac rhythm disorders. In 2002 over 300 000 units were sold in the United States and almost 900 000 worldwide. While the electronic pacemaker represents a tremendous therapeutic success, there are limitations that have generated interest in using gene- or cell-based therapies to develop a biological pacemaker. The potential advantages of a biological pacemaker include simple implantation via catheterization, elimination of the need to periodically replace the battery, and responsiveness to endogenous neuronal and hormonal signals.

Several approaches have been taken in developing a gene-based biological pacemaker. The first effort in this direction involved regional overexpression of the β_2-adrenergic receptor to enhance the normal chronotropic adrenergic responsiveness of myocardial tissue[1,2]. While not a true biological pacemaker in the sense of creating a pacemaker focus in non-pacing tissue, it nonetheless demonstrated the feasibility of modifying cardiac rhythm *in vivo* by means of gene therapy. Another approach overexpressed a dominant negative form of the inward rectifier K channel to reduce background outward current that normally opposes depolarizing inward currents[3]. While this approach resulted in a biological pacemaker (i.e. impulse initiation from a normally non-pacing cardiac region), the ionic basis of the pacemaker is subject to debate[4,5]. Further, reduction of a background K current such as the inward rectifier would be expected to impact net current flow at all voltages, resulting in a potentially pro-arrhythmic prolongation of action potential duration.

We have taken a different approach, overexpressing a member of the hyperpolarization-activated cyclic nucleotide gated (HCN) pacemaker channel gene family[6,7], which represents the molecular correlate of the cardiac pacemaker current (I_f). These channels are unique in activating on hyperpolarization, then deactivating rapidly on depolarization to positive potentials. These biophysical characteristics mean that inward current preferentially flows through these channels at negative potentials. Thus, if these channels are overexpressed they should contribute to a depolarizing current during diastole without affecting action potential plateau.

It should be noted that there is debate in the literature concerning the extent to which these channels actually contribute to normal cardiac pacemaking[8,9]. This debate centers on whether native channels are sufficiently activated at diastolic potentials, or require more negative voltages (i.e. voltages outside the relevant physiological range) for activation. What is clear, however, is that if overexpressed HCN channels yield a current of sufficient magnitude and with appropriate voltage- and time-dependence, they should result in generation of a diastolic depolarization and impulse initiation. Thus, the rationale for this approach is the hypothesis that if HCN channels are active at potentials near the resting potential when overexpressed in a particular target cell, the channels should initiate or accelerate pacemaking.

Initial validation of this hypothesis was provided in cell culture studies. These experiments took advantage of two key facts: 1) neonatal rat ventricular myocytes, when grown in monolayer culture, beat spontaneously; 2) I_f is present at only low density in these cells, but its activation voltage is near the normal resting potential. Thus, we reasoned that if pacemaker current could be overexpressed in these cells and exhibited biophysical characteristics similar to those of the native current, spontaneous rhythm would be enhanced. To test this prediction, we prepared an adenoviral construct containing the mouse HCN2 gene (AdHCN2), since this is the dominant HCN isoform at the message level in ventricular tissue[10]. We incorporated the gene into an adenovirus because neonatal ventricular cultures, when infected with adenovirus, express the carried genes with greater than 90% efficiency. We found that HCN2 overexpressing cultures exhibited a significantly greater spontaneous rhythm (88 ± 5 b/min) than control cultures (48 ± 4 b/min) that were infected with an adenovirus carrying the enhanced green fluorescent protein gene, AdGFP[11].

On the basis of this observation, we proceeded to test the ability of HCN2, when overexpressed *in vivo*, to generate an ectopic automatic focus. For these first *in vivo* studies we either injected AdHCN2 in combination with AdGFP, or injected AdGFP alone as control, into the myocardium of the canine left atrium[6]. We chose atrial tissue as the target because native I_f activates at less negative potentials in atrium than ventricle[12,13], and thus the expressed current would be more likely to be physiologically active. Further, canine atrium exhibits significantly less I_{K1} density than ventricle[14], and thus should have less stabilizing outward current at the resting potential to oppose the HCN-based diastolic depolarization. Atrial myocytes were isolated 3-4 days post-injection and GFP positive cells identified for patch-clamp recording. These experiments demonstrated that animals injected with AdHCN2 + AdGFP expressed a pacemaker current 500× greater than that of control atrial cells, and that this expressed current was active at physiological voltages. Specifically, activation threshold was ~ -75 mV and the midpoint of the activation relation was -95.2 ± 0.4 mV. This large pacemaker current in left atrial myocytes was associated with a left atrial ectopic focus when normal right atrial sinus node activity was suppressed by vagal stimulation (n = 4). In comparison, 3 animals that received only AdGFP did not exhibit a spontaneous atrial rhythm during vagal stimulation.

To apply this therapeutic approach to conditions of atrioventricular block it is necessary to deliver the gene below the atrioventricular node. We have done this in studies employing a catheter to inject AdHCN2 into the posterior division of the canine left bundle branch[7]. All AdHCN2 injected animals developed a left ventricular escape rhythm upon vagal stimulation, with mean escape rate significantly greater than that of AdGFP injected control animals. Thus, whether targeted to an atrial or Purkinje region, viral delivery of HCN2 genes to myocardial cells results in generation of large pacemaker currents and automatic rhythms localized to the site of injection.

An alternative approach to direct delivery of HCN or other genes to cardiac myocytes would be to introduce cells capable of either beating spontaneously or generating a large depolarizing current. In either case, these implanted cells would need to be electrically coupled to the surrounding myocardial tissue. One method of achieving this goal might be to implant embryonic stem cells that had differentiated in culture into a spontaneously active nodal type cardiac lineage, and recently a preliminary report of such an approach has appeared[15]. However, there are problems associated with the use of embryonic stem cells, including uniformity of differentiation, source availability and potential neopasticity. We therefore have been exploring a different technique using genetically engineered adult human mesenchymal stem cells (hMSC) available from bone marrow[16]. These cells have the advantage of being readily available and can be obtained from the patient for autologous transplantation, thereby eliminating any concerns of immunogenicity.

The rationale for this approach is that, if these cells are engineered to overexpress HCN genes and then couple to myocardial cells after implantation *in situ*, the surrounding cardiac tissue will hyperpolarize the hMSC to negative potentials that will activate the HCN channels. The resulting inward current flow into the hMSC will in turn depolarize the electrically coupled myocardium, leading to generation of an action potential in this tissue. The depolarization associated with the action potential will in turn depolarize the hMSC and deactivate the HCN channels. This situation differs from that of direct HCN expression in myocardial cells in that in this case the myocardial tissue is not made inherently automatic. Rather, the coupled hMSC act as a current source (entirely analogous to an electronic pacemaker) that flows into the myocardial cells and drives them to threshold. The unique biophysical characteristics of the HCN channels allow them to act as both a current source and a switch, in that the channels will only be open when the electrotonically coupled myocardium is in diastole. In this case, we injected hMSC expressing either HCN2 or enhanced GFP directly into the ventricular subepicardium. Upon vagal stimulation, mean escape rhythm was significantly greater in animals injected with HCN2-expressing hMSC than in those injected with GFP-expressing hMSC, and in the former case the escape rhythm always localized near the injection site.

In conclusion, I_f-based gene therapy, whether achieved by direct expression of HCN genes in myocardial cells or by expression in hMSC which are then implanted into the myocardium, is a feasible approach to creation of a biological pacemaker. Proof of concept experiments has clearly demonstrated the ability of such interventions to generate an ectopic focus that can drive the heart when normal sinus rhythm is suppressed. However, a number of issues remain to be addressed. One such issue is optimization of the expressed HCN gene in terms of both biophysical characteristics and neurohumoral responsiveness, so as to achieve a physiologically relevant and regulatable rhythm. Studies with different HCN isoforms and with channel mutations are likely to lead to improvements in this regard. In addition, selection of the proper promoter also may be important to achieve appropriate levels of expression. A final issue is the long-term persistence of the expressed gene. The initial viral studies have employed an adenoviral vector, which is not likely to persist for more than a few months *in vivo*. Therefore, alternate vectors may be needed to create a persistent pacemaker based on overexpression within myocardial cells. Persistence of expression is less likely to be an issue with hMSC-based pacemakers, if the implanted cells fully integrate into the cardiac syncytium.

References

1. Edelberg JM, Aird WC, Rosenberg RD. Enhancement of murine cardiac chronotropy by the molecular transfer of the human beta2 adrenergic receptor cDNA. J Clin Invest 1998; 101: 337-43.
2. Edelberg JM, Huang DT, Josephson ME, Rosenberg RD. Molecular enhancement of porcine cardiac chronotropy. Heart 2001; 86: 559-62.
3. Miake J, Marban E, Nuss HB. Gene therapy: biological pacemaker created by gene transfer. Nature 2002; 419: 132-3.
4. Silva J, Rudy Y. Mechanism of pacemaking I_{K1}-downregulated myocytes. Circ Res 2003; 92: 261-3.
5. Miake J, Nuss B. Multiple ionic conductances sustain I_{K1}-suppressed biopacemaking. (abstr) Circulation 2003; 108: IV-35.
6. Qu J, Plotnikov AN, Danilo PJ, et al. Expression and function of a biological pacemaker in canine heart. Circulation 2003; 107: 1106-9.
7. Plotnikov AN, Sosunov EA, Qu J, et al. A biological pacemaker implanted in the canine left bundle branch provides ventricular escape rhythms having physiologically acceptable rates. Circulation 2004, in press.
8. Irisawa H, Brown HF, Giles W. Cardiac pacemaking in the sinoatrial node. Physiol Rev 1993; 73: 197-227.
9. Accili EA, Proenza C, Baruscotti M, DiFrancesco D. From funny current to HCN channels: 20 years of excitation. News Physiol Sci 2002; 17: 32-7.
10. Shi W, Wymore R, Yu H, et al. Distribution and prevalence of hyperpolarization-activated cation channel (HCN) mRNA expression in cardiac tissues. Circ Res 1999; 85: E1-E6.
11. Qu J, Barbuti A, Protas L, et al. HCN2 over-expression in newborn and adult ventricular myocytes: distinct effects on gating and excitability. Circ Res 2001; 89: E8-E14.

12. Hoppe UC, Beuckelmann DJ. Characterization of the hyperpolarization-activated inward current in isolated human atrial myocytes. Cardiovasc Res 1998; 38: 788-801.
13. Hoppe UC, Jansen E, Sudkamp M, Beuckelmann DJ. Hyperpolarization-activated inward current in ventricular myocytes from normal and failing human hearts. Circulation 1998; 97: 55-65.
14. Melnyk P, Zhang L, Shrier A, Nattel S. Differential distribution of Kir2.1 and Kir2.3 subunits in canine atrium and ventricle. Am J Physiol 2002; 283: H1123-H1133.
15. Kehat I, Kheimovitz L, Gepstein A, et al. Generation of a biological pacemaker using human ES cell-derived cardiomyocytes. (abstr) Circulation 2003; 108: IV-35.
16. Plotnikov AN, Shlapakova IN, Danilo P Jr, et al. Human mesenchymal stem cells transfected with HCN2 as a gene delivery system to induce pacemaker function in canine heart. (abstr) Circulation 2003; 108: IV-547.

SPONTANEOUS ANIMAL MODELS OF ARRHYTHMOGENIC CARDIOMYOPATHIES

Cristina Basso

Institute of Pathology, University of Padua, Padua, Italy

According to the WHO/ISFC classification cardiomyopathies include heart muscle disease associated with cardiac dysfunction[1]. Among them, those characterized by a high incidence of ventricular arrhythmias even at risk of sudden death are represented by hypertrophic, arrhythmogenic right ventricular (ARVC) and inflammatory cardiomyopathies.

Several naturally occurring animal models of cardiovascular disease have as a consequence ventricular arrhythmias and sudden death. These include feline hypertrophic cardiomyopathy[2,3], ventricular arrhythmias associated with autonomic dysfunction in German shepherd dogs[4], left ventricular dysfunction in Doberman pinscher dogs[5], boxer cardiomyopathy[6,7] and feline ARVC, although sudden death was not the main feature in this spontaneous feline model[8,9].

The availability of spontaneous animal models, like in other types of cardiomyopathies, will contribute to gain an insight into the etiopathogenesis of the disease. In particular, ARVC has recently been found to occur spontaneously both in domestic cats and boxer dogs[8,9].

In cats, the prevalent clinical manifestations consisted of congestive heart failure, polymorphic ventricular arrhythmias including ventricular tachycardia and right bundle branch block[8]. Enlargement of the right ventricle and tricuspid regurgitation were detected at echocardiography. At autopsy the feline hearts were characterized by moderate-to-severe right ventricular enlargement and wall thinning with apical aneurysms in 50%. The left ventricle was focally involved in most of cases. Evidence of myocardial injury (myocyte death and atrophy) and repair (fibro-fatty replacement) in the setting of myocarditis and apoptosis was found at histology. These findings, similar to those described in human ARVC[10], were in keeping with an infective-inflammatory pathogenesis in this feline spontaneous model of ARVC.

Since many years, it has been noted that the boxer canine breed is predisposed to ventricular arrhythmias and sudden death[6,7], but the underlying disease responsible for these clinical features has been incompletely defined. We have recently documented a novel, spontaneous animal model of ARVC and sudden death in the boxer dog that is strikingly similar to clinical and pathologic features of the human condition[9]. The combined clinical profile (sudden death, ventricular arrhythmias of suspected right ventricular origin, and syncope) and pathologic abnormalities (right ventricular chamber enlargement and aneurysm, right ventricular myocyte loss and fatty replacement, myocarditis, and apoptosis) provide compelling evidence for this canine model. Furthermore, this represents another example of spontaneous and previously unrecognized heart disease in animals closely resembling the human condition.

Loss of right ventricular myocytes with replacement by fat or fibro-fatty tissue is the pathologic hallmark of human ARVC[10]. *Postmortem* magnetic resonance imaging accurately identified intramyocardial fat in the right ventricular locations confirmed by histopathology, suggesting that clinical recognition and assessment of disease progression is readily possible in this canine ARVC model.

Purely fatty replacement of right ventricular represented the predominant morphologic variant in two thirds of our boxer dogs, most substantially in the infundibular and anterolateral regions. In these dogs the right ventricular wall thickness remained normal and right ventricular aneurysms were uncommon. Although the fibro-fatty pattern of ARVC was present in one third of dogs in the present study, in contrast, it constitutes the predominant morphologic pattern in feline ARVC and is associated with extensive right ventricular myocardial loss, replacement fibrosis, and correspondingly, frequent wall thinning and right ventricular aneurysms[8]. This latter association between fibro-fatty replacement and right ventricular wall thinning and aneurysmal formation is most similar to that observed in patients with ARVC[10,11].

While the precise role of myocarditis and apoptosis in the pathogenesis of ARVC is unresolved, findings of this study support the view that these processes modulate disease morphology and progression. Some investigators consider fatty and fibro-fatty patterns as consecutive stages of disease, mediated by myocarditis, in which the fatty form is an early feature and fibro-fatty repair results from myocarditis-induced injury[10,11]. Consistent with this hypothesis, right ventricular inflammatory infiltrates were pronounced in boxer dogs with the fibro-fatty form, whereas areas of myocarditis were small and uncommon when associated with purely fatty

replacement. It is also noteworthy that in the feline model of ARVC, right ventricular myocarditis was also a characteristic feature in the fibro-fatty pattern[9]. Furthermore, our finding of apoptotic myocytes in boxer dogs with ARVC is consistent with the hypothesis that loss of right ventricular myocardial cells and replacement by fat and fibrosis is mediated by programmed cell death[11].

As with young ARVC patients who die suddenly[10,11], the presence of diffuse right ventricular myocyte loss, fatty replacement, and residual myocytes embedded within fat, as well as myocarditis, in our boxer dogs suggest a substrate predisposed to sudden death.

In the boxer dogs ARVC occurred in siblings, parents, and offspring, indicating familial transmission. We did not, however, systematically study those pedigrees and therefore, the precise inheritance pattern remains unresolved. Nevertheless, examples of transmission from one generation to another suggest the likelihood of dominant inheritance which, in turn, would be consistent with that of the human disease. Of note, Meurs et al.[7] reported autosomal dominant inheritance in boxer dogs with ventricular arrhythmias. Although undocumented, it is possible that the familial occurrence of ventricular arrhythmias in such dogs was a marker for ARVC.

In conclusion, novel, spontaneous animal models of ARVC both in cats (right ventricular failure) and in boxer dogs (sudden death) which closely resemble the clinical and pathologic features of the human disease have been reported. In addition to sudden death, the canine model is characterized by ventricular tachycardia of suspected right ventricular origin, and structural right ventricular abnormalities distinguished by right ventricular enlargement, myocyte loss with fatty or fibro-fatty replacement, myocarditis, and apoptosis. Several of these dogs were related, suggesting that canine ARVC is inherited. These animal models of human ARVC constitute a new and potentially useful investigative tool to understand the complex clinical and pathogenic mechanisms responsible for sudden death and disease progression.

References

1. Richardson P, McKenna W, Bristow M, et al. Report of the 1995 World Health Organization/International Society and Federation of Cardiology Task Force on the definition and classification of cardiomyopathies. Circulation 1996; 93: 841-2.
2. Fox PR, Liu SK, Maron BJ. Echocardiographic assessment of spontaneously occurring feline hypertrophic cardiomyopathy. An animal model of human disease. Circulation 1995; 92: 2645-51.
3. Kittleson MD, Meurs KM, Munro MJ, et al. Familial hypertrophic cardiomyopathy in Maine coon cats: an animal model of human disease. Circulation 1999; 99: 3172-80.
4. Moise NS, Meyers-Wallen V, Flahive WJ, et al. Inherited ventricular arrhythmias and sudden death in German shepherd dogs. J Am Coll Cardiol 1994; 24: 233-43.
5. Calvert CA, Hall G, Jacobs G, et al. Clinical and pathologic findings in Doberman pinschers with occult cardiomyopathy that died suddenly or developed congestive heart failure: 54 cases (1984-1991). J Am Vet Med Assoc 1997; 210: 505-11.
6. Harpster NK. Boxer cardiomyopathy. In: Kirk RW, ed. Current veterinary therapy. Philadelphia, PA: WB Saunders, 1983: 329-37.
7. Meurs KM, Spier AW, Miller MW, et al. Familial ventricular arrhythmias in boxers. J Vet Intern Med 1999; 13: 437-9.
8. Fox PR, Maron BJ, Basso C, et al. Spontaneous occurrence of arrhythmogenic right ventricular cardiomyopathy in the domestic cat: a new animal model of human disease. Circulation 2000; 102: 1863-70.
9. Basso C, Fox P, Meurs K, et al. Arrhythmogenic right ventricular cardiomyopathy causing sudden cardiac death in boxer dogs: a new animal model of human disease. Circulation 2004, in press.
10. Basso C, Thiene G, Corrado D, et al. Arrhythmogenic right ventricular cardiomyopathy. Dysplasia, dystrophy, or myocarditis? Circulation 1996; 94: 983-91.
11. Thiene G, Basso C. Arrhythmogenic right ventricular cardiomyopathy. An update. Cardiovasc Pathol 2001; 10: 109-17.

SMOKING AND SUDDEN INFANT DEATH SYNDROME: ELECTROPHYSIOLOGICAL INSIGHTS FROM AN EXPERIMENTAL MODEL

Laura Sartiani, Francesca Stillitano, Raffaele Paola, Giuseppe Lonardo, Simona Brogioni, Elisabetta Cerbai, Alessandro Mugelli

Center of Molecular Medicine (CIMMBA), University of Florence, Florence, Italy

Maternal smoking is a risk factor for sudden infant death syndrome. Although the association between sudden infant death syndrome and maternal smoking is well established, its rational basis is largely ignored. In particular, no information is available concerning the effect of carbon monoxide (CO, a component of smoke) on postnatal maturation of the heart. We postulated that prenatal exposure to CO may affect the postnatal development of cardiovascular system, and particularly the electrophysiological maturation of the neonatal rat heart. Such an effect may predispose to the appearance of congenital electrical instability and arrhythmias. The effect of prenatal exposure to CO on the cellular electrophysiological maturation of ventricular rat myocytes was studied by means of the patch-clamp technique; reverse transcriptase-polymerase chain reaction was used to evaluate mRNA expression. Physiological cell growth of ventricular myocytes and fall in atrial natriuretic peptide expression were similar in the two groups over the first 2 months of life. However, the age-related shortening in action potential duration was significantly delayed in CO-exposed rats. This phenomenon might result in prolonged repolarization in the early phase of life, favoring the occurrence of life-threatening arrhythmias.

Introduction

Sudden infant death syndrome (SIDS) is the major cause of unexpected death during the first year of life. Many modifiable risk factors have been recognized and educational campaigns have successfully reduced the incidence of SIDS. As a multifactorial disease, likely determined by the contribution of genetic and environmental factors, its understanding and prevention remain incomplete. Among the potential causes, smoking during pregnancy represents a major independent risk factor which requires increased attention.

Cigarette smoke contains a 4% carbon monoxide (CO), which easily crosses the placental barrier increasing carboxyhemoglobin levels in umbilical cord blood[1]. Chronic fetal hypoxia may alter the physiological development of tissues, especially those more susceptible to hypoxia damage such as the brain[2]. Indeed, alterations in the autonomic nervous system in infants from smoking mothers have been reported[3].

Recent electrocardiographic and genetic studies in newborns suggest that congenital long QT syndrome may account for some cases of SIDS[4]. Congenital mutations for the sodium channels have been linked to fatal and non-fatal cardiac events in neonates with long QT[5-8]. However, the epidemiological relevance of SIDS suggests that environmental (and modifiable) factors may strengthen and extend beyond the genetic predisposition to QT prolongation and cardiac death. In this perspective, the effect of smoking and its constituents on the developing heart has received little attention.

Electrophysiological and hormonal properties of the developing heart change dramatically during the first weeks of life. Cardiac maturation is accompanied by a progressive shortening of the QT interval, documented in humans[9], dogs[10], and rats[11,12]. Neurohumoral and hormonal signals (sympathetic innervation, thyroid hormone) seems to play a key role in these changes, since their deficiency causes an abnormally prolonged repolarization[13,14]. At the same time, the ventricular synthesis of atrial natriuretic peptide (ANP) falls rapidly over the first 2 weeks after birth[15,16] and its re-expression consistently occurs as a result of pathological cardiac hypertrophy and failure[16].

Here we extend a previous report demonstrating that prenatal exposure to CO levels alters the physiological maturation of cardiac cellular properties, likely predisposing to neonatal arrhythmias[17]. This effect was observed at a CO concentration (150 ppm), resulting in blood levels of carboxyhemoglobin comparable to those found in human cigarette smokers[2].

Methods

Animal treatment. Pregnant primiparous Wistar female rats are exposed to 0 or 150 ppm CO mixed with air throughout the time of pregnancy, as reported elsewhere[2,18]. At birth, litters are reduced to six male pups. From 1 to 60 days of life, one control and one CO-exposed male rats are sacrificed at any experimental time, in order to maintain litter homogeneity.

Cell isolation. Neonatal cardiomyocytes are isolated following a previously published procedure[19]. The same method is used on hearts from control and CO-exposed rats and independently of animal age to have homogeneous conditions. At any age, ventricular samples are collected from control and CO-treated rats and immediately frozen in liquid nitrogen for total RNA extraction and reverse transcriptase-polymerase chain reaction (RT-PCR) assays of mRNA expression.

Patch-clamp experiments. Electrophysiological properties (membrane capacitance, action potentials) of the isolated myocytes are measured by means of the patch-clamp technique in the whole cell configuration[19].

Reverse transcriptase-polymerase chain reaction. Total RNA was extracted from tissue using a Qiagen kit. The total RNA was separated by gel electrophoresis and spectrophotometry at 260 and 280 nm was performed to measure the amount and quality of RNA. The RNA was converted to cDNA by reverse transcription and standard PCR carried out using 100 ng cDNA and primers directed against the rat sequence for ANP. Primers for GAPDH are added for co-amplification in each sample as an internal control for mRNA integrity and equal loading. PCR was carried out by using 30 cycles of amplification, which shown results in the exponential phase of amplification for these genes. The amplified mixture (5 μl) was separated by electrophoresis; bands detected using ethidium bromide staining, were photographed under UV light and quantified with image analyzer (Scion Image).

Results and discussion

We analyzed three key parameters which are expected to change during postnatal maturation: cell size, ANP expression, and action potential profile. Figure 1A shows the average values of membrane capacitance, an index of cell size, measured in single ventricular myocytes from control or CO-exposed rats during aging. The expected increase in cell size was similar in the two groups. As previously reported, the synthesis of ANP by ventricular rat cells decreases physiologically during the first 2 weeks of life[16]. This phenomenon is paralleled by the decrease in mRNA transcription, as shown in figure 1B. The blot reports examples of mRNA expression in control rat hearts at different days after birth (from 2 to 35); a clear-cut band corresponding to ANP is visible at 2 to 12 days but it disappears afterward. Figure 1C compares the mRNA expression of ANP in ventricular samples of age-matched rats, showing that no differences

were observed between the two groups. Taken together, these data suggest that, from a morphological and biochemical point of view, postnatal hypertrophic growth of the heart is similar in control and CO-exposed rats.

Action potential duration undergoes a physiological shortening during cardiac maturation[11,12]. Figure 2A shows two action potentials recorded from a control ventricular myocyte compared with that recorded from a myocyte isolated from a CO-treated rat at 1 month. It is apparent that the most striking change regards the duration of the action potential, with that from ventricular myocytes isolated from the CO-exposed rat being markedly prolonged. This was confirmed by statistical analysis of data (Fig. 2B). No difference was observed in the youngest rats (2 weeks), where action potential duration measured at -50 mV was similarly prolonged. At 1 month of age, action potential duration physiologically shortened in control but not in CO-exposed rats, where it resulted to be significantly longer than in controls. At 2 months, action potential duration was reduced also in CO-exposed rats and not significantly different from that measured in controls.

Maternal smoking and sudden infant death syndrome: an arrhythmogenic basis? These data suggest that in rats, postnatal cardiac development is specifically influenced by prenatal exposure to CO. In particular, CO does not alter ventricular cell growth and fall in ANP synthesis. However, the physiological shortening of action potential duration is significantly delayed with respect to controls. Lengthening QT interval and action potential repolarization is considered a major risk for the occurrence of ventricular arrhythmias in several pathological conditions typical of the adulthood[20]. However, clinical observations suggest that long QT may represent a risk marker also for sudden cardiac

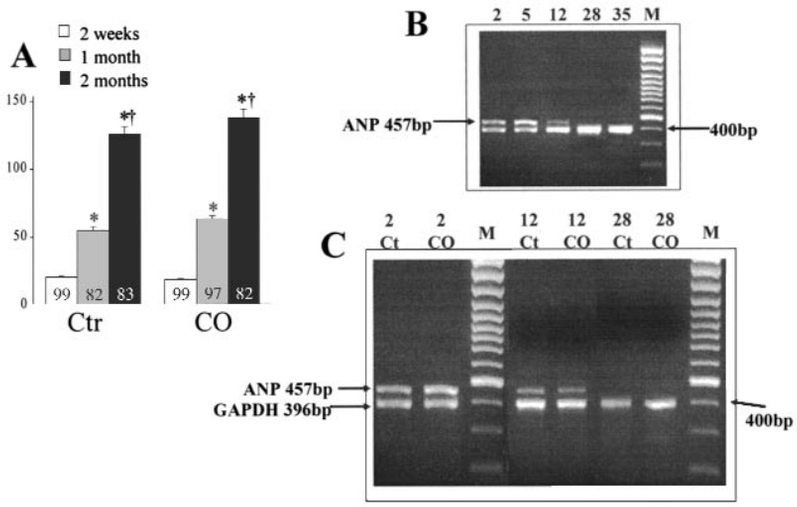

Figure 1. Panel A: *membrane capacitance, an index of cell size, during postnatal development in control (Ctr) and carbon monoxide (CO)-treated rat. Histograms are mean ± SEM values of the number of cells indicated on each column.* Panel B: *blot showing the mRNA bands obtained by reverse transcriptase-polymerase chain reaction for atrial natriuretic peptide and GAPDH in control rats at different days after birth (numbers above columns).* Panel C: *comparison of bands for atrial natriuretic peptide mRNA in ventricular homogenates from control (Ct) and CO-treated rats; numbers represent the age (in days) after birth. * p < 0.05 vs 2 week-old rats; † p < 0.05 vs 1 month-old rats.*

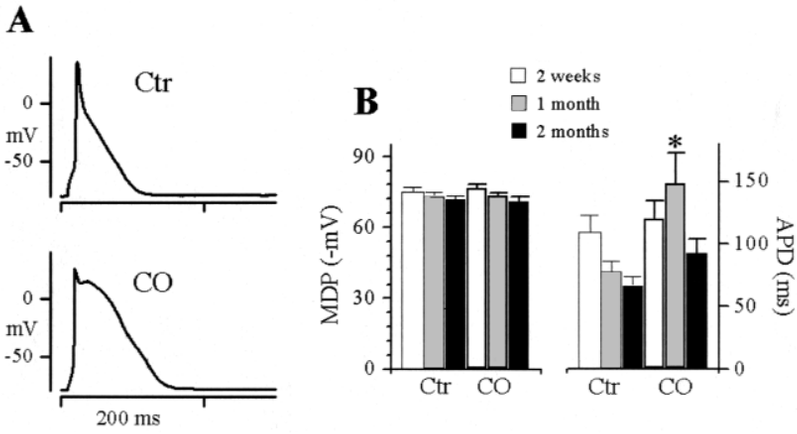

Figure 2. Panel A: *action potentials recorded from ventricular myocytes from control (Ctr,* top*) and carbon monoxide (CO)-treated rats* (bottom) *at 1 month of age.* Panel B: *summary of mean ± SEM values for maximum diastolic potential (MDP) and action potential duration (APD). * p < 0.05 vs age-matched controls.*

death in newborns[9]. Even if debated, some cases of SIDS have been associated with QT interval prolongation[4] and a genetic basis has been proposed following the observation of long QT syndrome mutations in these patients[5-7]. A speculative extrapolation of our findings to humans suggests that prolonged myocyte repolarization induced by environmental factors, such as prenatal exposure to smoke, might establish a period of vulnerability for life-threatening arrhythmias in newborns.

Acknowledgments

This study was supported by a grant from Scottish Cot Death Trust and Telethon no. GP0274-01. Animal treatment was performed by Drs. M. Tattoli, R. Cagiano and M.R. Carratù from the Department of Pharmacology, University of Bari, Italy. We thank Prof. V. Cuomo for helpful discussion.

References

1. Aubard Y, Magne I. Carbon monoxide poisoning in pregnancy. BJOG 2000; 107: 833-8.
2. Mereu G, Cammalleri M, Fa M, et al. Prenatal exposure to a low concentration of carbon monoxide disrupts hippocampal long-term potentiation in rat offspring. J Pharmacol Exp Ther 2000; 294: 728-34.
3. Browne CA, Colditz PB, Dunster KR. Infant autonomic function is altered by maternal smoking during pregnancy. Early Hum Dev 2000; 59: 209-18.
4. Schwartz PJ, Stramba-Badiale M, Segantini A, et al. Prolongation of the QT interval and the sudden infant death syndrome. N Engl J Med 1998; 338: 1709-14.
5. Schwartz PJ, Priori SG, Dumaine R, et al. A molecular link between the sudden infant death syndrome and the long QT syndrome. N Engl J Med 2000; 343: 262-7.
6. Schwartz PJ, Priori SG, Bloise R, et al. Molecular diagnosis in a child with sudden infant death syndrome. Lancet 2001; 358: 1342-3.
7. Ackerman MJ, Siu BL, Sturner WQ, et al. Postmortem molecular analysis of SCN5A defects in sudden infant death syndrome. JAMA 2001; 286: 2264-9.
8. Wedekind H, Smits JPP, Schulze-Bahr E, et al. De novo mutation in the SCN5A gene associated with early onset of sudden infant death. Circulation 2001; 104: 1158-64.
9. Schwartz PJ, Montemerlo M, Facchini M, et al. The QT interval throughout the first 6 months of life: a prospective study. Circulation 1982; 66: 496-501.
10. Jeck CD, Boyden PA. Age-related appearance of outward currents may contribute to developmental differences in ventricular repolarization. Circ Res 1992; 71: 1390-403.
11. Guo W, Kamiya K, Toyama J. Modulated expression of transient outward current in cultured neonatal rat ventricular myocytes: comparison with development in situ. Cardiovasc Res 1996; 32: 524-33.
12. Guo W, Kamiya K, Cheng J, Toyama J. Changes in action potentials and ion currents in long-term cultured neonatal rat ventricular cells. Am J Physiol 1996; 271 (Part 1): C93-C102.
13. Malfatto G, Rosen TS, Steinberg SF, et al. Sympathetic neural modulation of cardiac impulse initiation and repolarization in the newborn rat. Circ Res 1990; 66: 427-37.
14. Shimoni Y, Fiset C, Clark RB, Dixon JE, McKinnon D, Giles WR. Thyroid hormone regulates postnatal expression of transient K^+ channel isoforms in rat ventricle. J Physiol 1997; 500 (Part 1): 65-73.
15. Wei YF, Rodi CP, Day ML, et al. Developmental changes in the rat atriopeptin hormonal system. J Clin Invest 1987; 79: 1325-9.
16. Gutkowska J, Nemer M. Structure, expression, and function of atrial natriuretic factor in extraatrial tissues. Endocr Rev 1989; 10: 519-36.
17. Sartiani L, Cerbai E, Lonardo G, et al. Prenatal exposure to carbon monoxide affects postnatal cellular electrophysiological maturation of the rat heart: a potential substrate for arrhythmogenesis in infancy. Circulation, in press.
18. Carratu MR, Cagiano R, Desantis S, et al. Prenatal exposure to low levels of carbon monoxide alters sciatic nerve myelination in rat offspring. Life Sci 2000; 67: 1759-72.
19. Cerbai E, Pino R, Sartiani L, Mugelli A. Influence of postnatal-development on if occurrence and properties in neonatal rat ventricular myocytes. Cardiovasc Res 1999; 42: 416-23.
20. Tomaselli G, Marban E. Electrophysiological remodeling in hypertrophy and heart failure. Cardiovasc Res 1999; 42: 270-83.